4

Results

The results pertaining to the study entitled **"Comparative Evaluation of Liposome Encapsulated *Hygrophila auriculata* (Schumach.) Heine Root and Betulin on Wound Healing Activity through *In silico, In vitro* and *In vivo* approaches"** are presented under the following headings:

PHASE I

4.1. Preliminary phytochemical analysis and antioxidant studies

4.1.1. Physicochemical analysis

The results of the physicochemical parameters of the root and leaves of *H.auricualata* are depicted in table III.

Table III. Physicochemical parameters of *H. auriculata* leaves and roots

Physicochemical parameters		Roots	leaves
Physical characters	Color	Brown	Olive green
	Odour	Aromatic	Aromatic
	Taste	Bitter	Bitter
Moisture content (%)	Loss on drying	0.42	0.54
Ash value (%)	Total ash value	4.17	3.24
	Acid insoluble ash	2.81	3.66
	Water soluble ash	3.26	4.46

4.1.2. Qualitative Phytochemical screening

A qualitative phytochemical analysis was performed on the root and leaves of *H.auriculata* to detect the major phytochemicals. The findings revealed the existence of alkaloids, flavonoids, phenols, tannins, proteins, carbohydrates, cardiac glycosides, and terpenoids with the highest intensity observed in the ethanol extract in both the leaves and roots. Table IV. provides an overview of the presence or absence of different phytochemicals.

Table IV. Qualitative analysis of the primary and secondary metabolites of *H. auriculata*

S. No.	Phytochemicals	Leaves				Roots			
		Chloroform	Ethanol	Ethyl acetate	Aqueous	Chloroform	Ethanol	Ethyl acetate	Aqueous
1.	Alkaloids	+	+	+	-	+	+	+	-
2.	Flavonoids	+	+	+	+	+	+	+	+
3.	Sterols	-	-	-	+	-	-	-	+
4.	Phenols	-	+	+	-	-	+	+	-
5.	Saponins	-	-	+	-	-	-	+	-
6.	Tannins	+	+	+	-	+	+	+	-
7.	Quinones	-	-	-	-	-	-	-	-
8.	Proteins	+	+	-	+	+	+	-	+
9.	Carbohydrates	-	+	-	+	-	+	-	+
10.	Cardiac glycosides	-	+	-	+	-	+	-	+
11.	Terpenoids	-	+	-	+	-	+	-	+

+-→ presence of the phytochemical; -- → absence of the phytochemical

4.1.3. Free radical scavenging activities

The leaves and roots of *H. auriculata* of different extracts were subjected to the *in vitro* radical scavenging activities against a battery of radicals namely DPPH, ABTS, and ferric reducing antioxidant power assay.

4.1.3.1. DPPH assay

In the DPPH assay, the extent of DPPH scavenging by all the extracts was significant, where the stable radical was effectively reduced to the yellow-coloured compound di phenylpicryl hydrazine. Among the four solvents used the ethanol extract of leaves and roots of *H. auriculata* has the highest free radical scavenging capacity with an IC_{50} value of 75 µg/ml and 67 µg/ml followed by ethyl acetate extract. The least activity was shown by chloroform extract. The results are presented in Fig. 7.

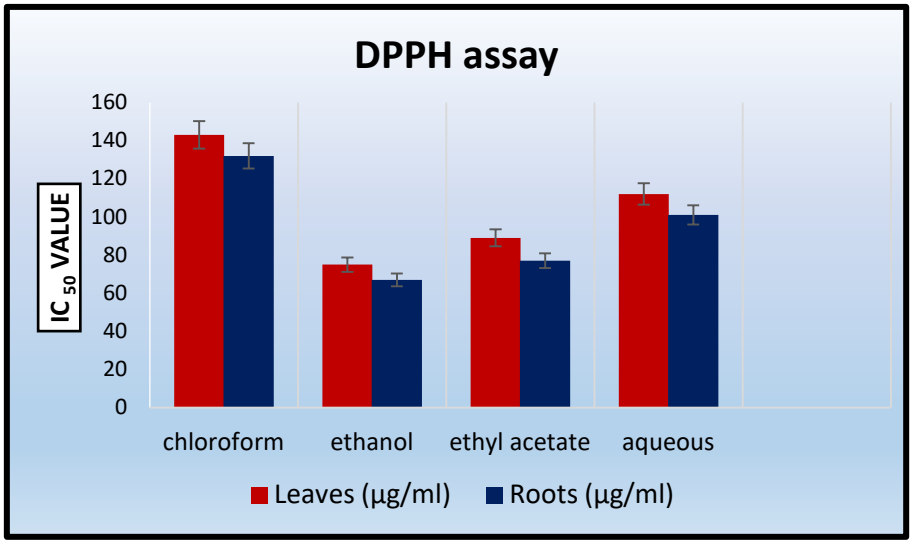

Fig. 7. DPPH assay of leaves and roots of *H. auriculata*

4.1.3.2. ABTS assay

The radical scavenging activity of the leaves and roots of *H. auriculata* were analyzed using ABTS radical are shown in Fig.8. It was observed that the different solvent extracts effectively scavenged the ABTS free radicals. The extent of ABTS radical scavenging was higher in the ethanol extract in the leaves and roots of *H. auriculata* followed by the ethyl acetate and aqueous extracts. The IC_{50} value of ethanol extract of the leaves and roots of *H. auriculata* were 77 µg/ml and 70 µg/ml. The chloroform extract showed the lowest effect.

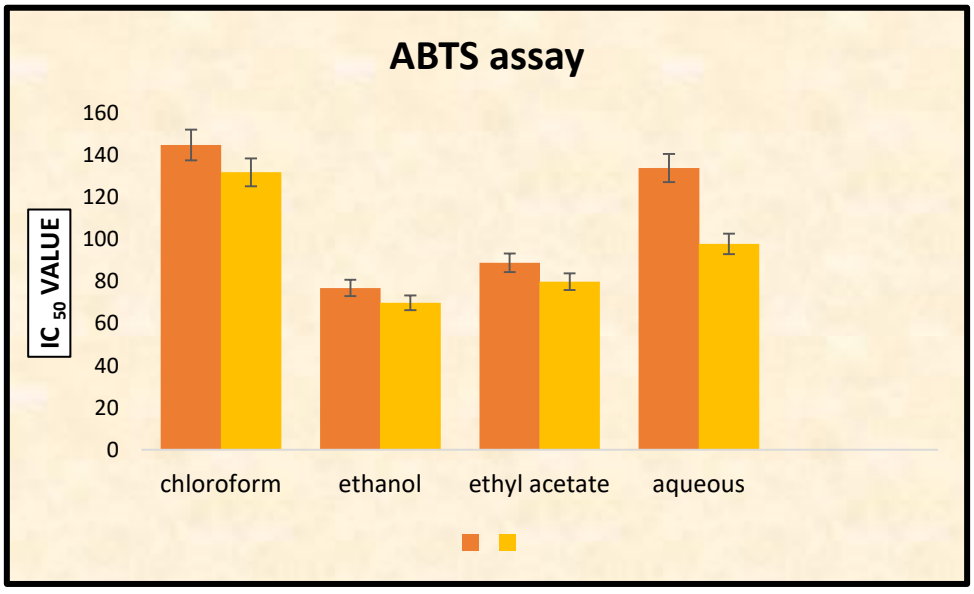

Fig. 8. ABTS assay of leaves and roots of *H. auriculata*

4.1.3.3. FRAP assay

The reducing capacity of a compound serves as a significant indicator of its antioxidant capacity. The presence of reductants in all the extracts resulted in the reduction of ferric cyanide complex to ferrous form with the development of Perl's Prussian blue. This can be monitored at an absorbance of 700 nm and found that the ethanol extract of the leaves and roots of *H. auriculata* showed highest reductive capability (Fig. 9).

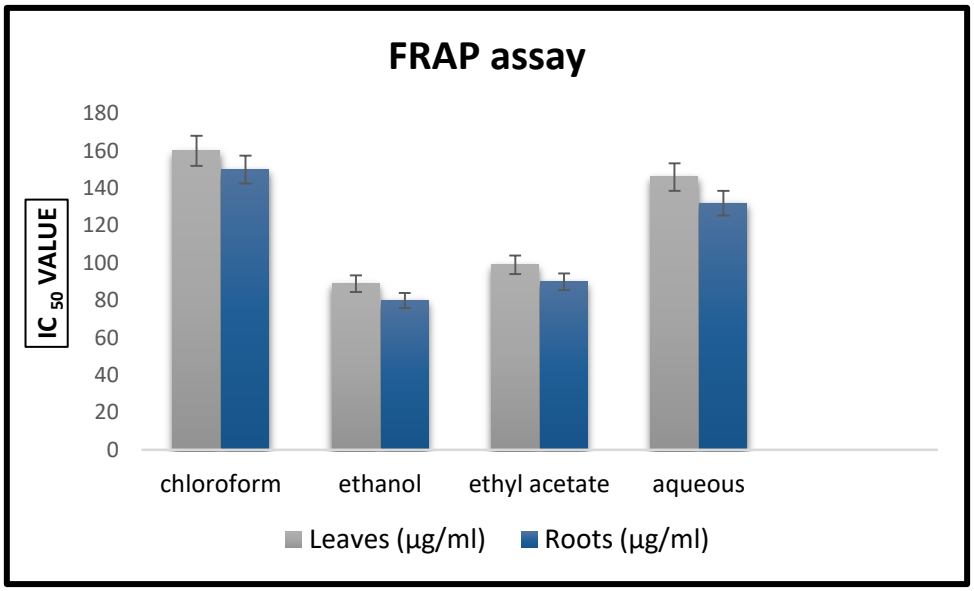

Fig. 9. FRAP assay of leaves and roots of *H. auriculata*

4.1.4. Antioxidant activity

The results of the free radical scavenging assays showed that the ethanol extract of leaves and roots of *H. auriculata* exhibited the highest free radical scavenging activity in cell free systems. Hence antioxidant activity of the ethanol extract of leaves and roots of *H. auriculata* was analysed by evaluating the enzymic and non-enzymic parameters.

4.1.4.1. Enzymatic and non-enzymatic antioxidant activity

The activities of enzymic SOD (superoxide dismutase), POD (peroxidase), CAT (catalase), Polyphenol oxidase and GST (glutathione S transferase) and non enzymic (flavonoids, α-tocopherol and vitamin – C) antioxidants were analysed.

Table V. depicts the levels of enzymic and non-enzymic antioxidants. SOD and POD in leaves and roots were found to be 11.5 ± 0.7, 13.3 ± 0.5 and 6.11 ± 7.33, 9.34 ± 2.11 U/mg respectively. In this study the catalase level was found to be 1.03 ± 0.5 and 4.53 ± 0.9 U/mg

and polyphenol oxidase was found to be 0.1 ± 0.01 and 0.4 ± 0.01 µg/g. The level of GST was 1.8 ± 0.1 and 2.3 ± 0.5 µg/g.

The level of non-enzymic antioxidants is also shown in Table V. Of the three enzymes analysed, the level of flavonoids was found to be 1.36 ± 0.53, 2.40 ± 1.23 µg/g in leabes and roots respectively. The level of α-tocopherol was found to be 26.5 ± 1.97 and 32.3 ± 0.18 µg/g and Vitamin – C were found to be 1.88 ± 0.12 and 2.93 ± 0.02 µg/g.

Among the leaves and roots of *H. auriculata* the ethanol extract of the roots of *H. auriculata* was found have maximum amount of enzymic and non-enzymic antioxidants.

Table V. Enzymatic and Non-enzymic antioxidant activity of *H. auriculata* leaves and roots

Levels of antioxidants	Leaves	Roots
Enzymatic antioxidants		
SOD (Units/mg)	11.5 ± 0.7	13.3 ± 0.5
POD (Units/mg)	6.11 ± 7.33	9.34 ± 2.11
CAT (Units/mg)	1.03 ± 0.5	4.53 ± 0.9
Polyphenol oxidase (µg/g)	0.1 ± 0.01	0.4 ± 0.01
GST (µg/g)	1.8 ± 0.1	2.3 ± 0.5
Non-enzymatic antioxidants		
Flavonoids (µg/g)	1.36 ± 0.53	2.40 ± 1.23
α – tocopherol (µg/g)	26.5 ± 1.97	32.3 ± 0.18
Vitamin – C (µg/g)	1.88 ± 0.12	2.93 ± 0.02

Values are expressed as mean ± SD of triplicates

Unit: SOD: Amount of enzyme that gives 50% reduction in NBT oxidation, POD: Change of absorbance/minute at 430 nm, CAT: Amount of enzyme required to decrease the absorbance at 240 nm by 0.5 units

Upon conducting preliminary research on the leaves and roots of *H. auriculata*, encompassing its phytochemical and antioxidant properties, it has been ascertained that the root component exhibits significant biological properties, which justify the need for further investigation. This valuable insight will aid in realizing the complete potential of the root for its wound healing properties.

PHASE II

4.2. *In silico* studies

4.2.1. LCMS analysis of *H. auriculata* root

The bioactive compounds of the *H. auriculata* root were qualitatively characterized by LCMS analysis in both positive (+) and negative (-) modes. In the present study, the protonated [M+H] + and deprotonated [M−H] − molecules of various phytoconstituents were revealed in the positive and negative ion modes (Fig. 10). The phyto compounds are listed in Table VI. The identified compounds belong to secondary metabolites like terpenoids, alkaloids, aliphatic compounds, and phenolic.

Table VI. The phytocompounds identified using LC-MS analysis

S. No.	Compound name	Molecular formula	Molecular weight (g/mol)	m/z	Mode (+/-)
1.	Caffeic anhydride	$C_{15}H_{18}O_9$	342	341.12	-
2.	Quercetin	$C_{15}H_{10}O_7$	302.24	301.03	-
3.	Myristic acid	$C_{14}H_{28}O_2$	228.37	227.37	-
4.	Palmitic acid	$C_{16}H_{32}O_2$	256.42	255.70	-
5.	1,3-Dicaffeoylquinic acid	$C_{25}H_{24}O_{12}$	516.4	515.05	-
6.	Coumaroyl quinic acid	$C_{16}H_{18}O_8$	338.31	337.12	-
7.	Epiafzelechin	$C_{15}H_{14}O_5$	274.27	273.78	-
8.	Kaempferol-7-O-Glucoside	$C_{21}H_{20}O_{11}$	447.4	446.76	-
9.	Betulin	$C_{30}H_{50}O_2$	442.72	443.45	+
10.	Linoleic acid	$C_{18}H_{32}O_2$	280.45	281.13	+
11.	Luteolin 7-O-rutinoside	$C_{27}H_{30}O_{16}$	610.52	611.36	+
12.	4 Feruloyl-5-caffeoylquinic acid	$C_{26}H_{26}O_{12}$	530.5	531.99	+
13.	Chlorogenic acid	$C_{16}H_{18}O_9$	354.3	355.67	+
14.	Myricetin-3-O-hexoside	$C_{21}H_{20}O_{13}$	480.4	481.24	+
15.	Apigenin-6-C-glucoside 8C-arabinoside	$C_{26}H_{28}O_{14}$	564.49	563.11	-

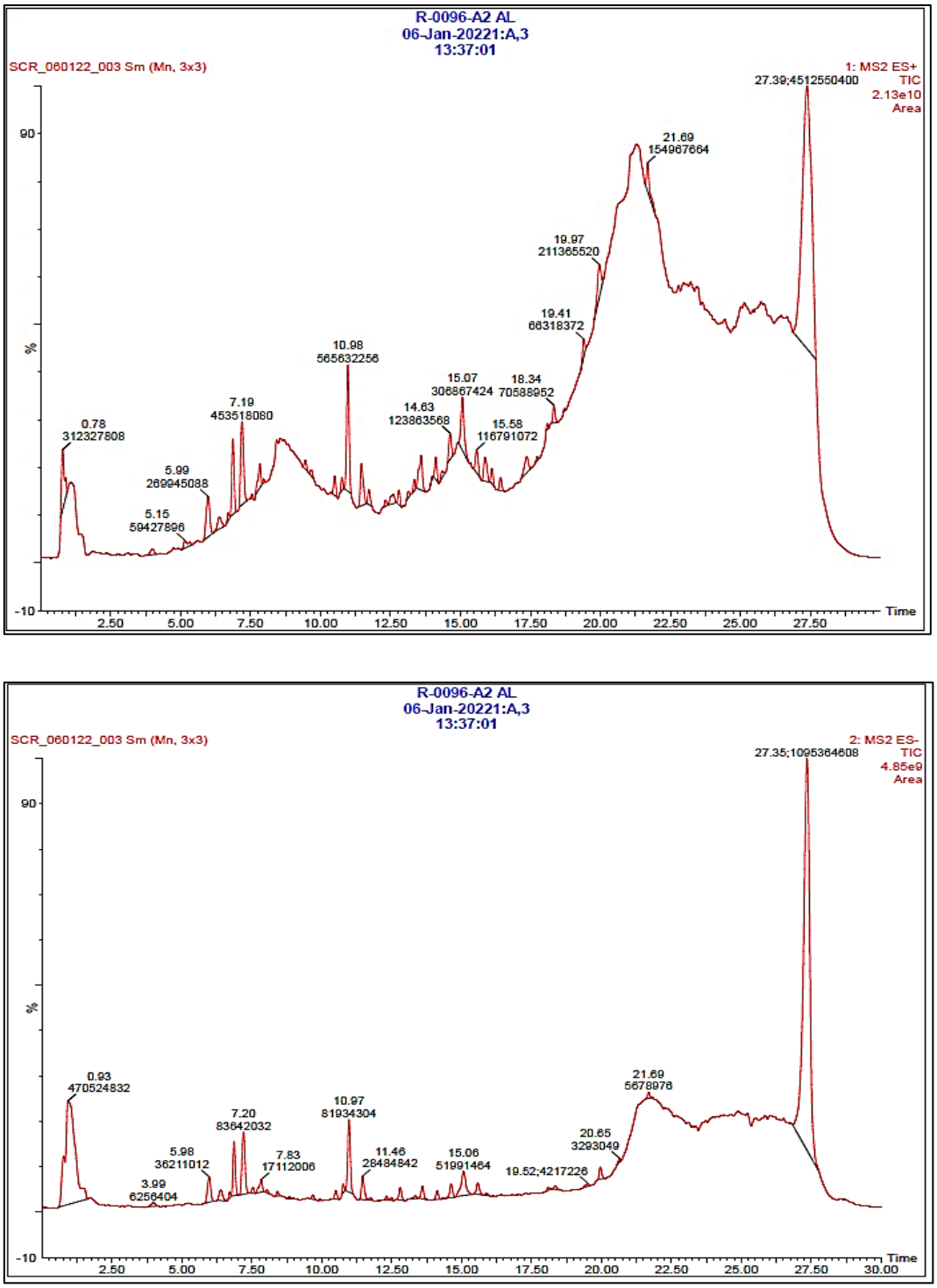

Fig.10. LC-MS spectrum of *H. auriculata* root

4.2.2. Selection of ligands from LCMS profile

The bioactive compounds with their molecular weight present in *H. auriculata* root identified by LC-MS analysis was reported in the chromatogram (Fig.10). The resulting LC-MS from *H. auriculata* root has totally 15 molecules. The spectrum profile of the LC-MS data of *H. auriculata* was verified with the PUBCHEM database. These compounds were

further chosen for *in silico* docking analysis with the target proteins responsible for the pathogenesis of wound.

4.2.3. Pubchem

PubChem is a huge database for small molecule deposition from NMR and XRD derived structures. The structure of fifteen molecules which had CAS numbers was collected from the PubChem database. The detail of the selected compounds was given in the Table VII.

Table VII. Ligands chosen for docking

S. No	Molecules	CAS number	Compounds	MW g/mol
1.	Caffeic anhydride	501-16-6	$C_{18}H_{14}O_7$	342
2.	Quercetin	117-39-5	$C_{15}H_{10}O_7$	302.23
3.	Myristic acid	544-63-8	$C_{14}H_{28}O_2$	228.37
4.	Palmitic acid	57-10-3	$C_{16}H_{32}O_2$	256.42
5.	1,3-Dicaffeoylquinic acid	19870-46-3	$C_{25}H_{24}O_{12}$	516.4
6.	Coumaroyl quinic acid	93451-44-6	$C_{16}H_{18}O_8$	338.31
7.	Epiafzelechin	24808-04-06	$C_{15}H_{14}O_5$	274.27
8.	Kaempferol-7-O-Glucoside	16290-07-6	$C_{21}H_{20}O_{11}$	447.4
9.	Betulin	473-98-3	$C_{30}H_{50}O_2$	442.72
10.	Linoleic acid	60-33-3	$C_{18}H_{32}O_2$	280.45
11.	Luteolin 7-O-rutinoside	20633-84-5	$C_{27}H_{30}O_{16}$	610.52
12.	4 Feruloyl-5- caffeoylquinic acid	125132-81-2	$C_{26}H_{26}O_{12}$	530.5
13.	Chlorogenic acid	327-97-9	$C_{16}H_{18}O_9$	354.3
14.	Myricetin-3-O-hexoside	19833-12-6	$C_{21}H_{20}O_{13}$	480.4
15.	Apigenin-6-C-glucoside 8C arabinoside	38953-85-4	$C_{26}H_{28}O_{14}$	564.49

4.2.4. Drug likeliness

The drug likeness properties of the 15 compounds were assessed by using Swiss ADME. Out of 15 molecules, only 10 molecules were found to satisfy drug like properties based on Lipinski's rule of five. Lipinski's rule of five defines a molecule as drug like only if the molar weight (MW) is less than 500 Daltons (Da); the logarithm of the octanol/water partition coefficient (Q PlogPo/w) is less than 5, the number of hydrogen bond acceptors (HBA) less than10 and the number of hydrogen bond donors (HBD) less than 5. The

distributions of the compound MW, log P, HBA and HBD were calculated and used to assess the likely drug like nature of the compounds derived from *H. auriculata* root (Table VIII).

Table VIII. Compliance of compounds to computational parameters of drug likeness (Lipinski's rule of five)

S. No.	Molecule	Molecular formula	MW (g/mol)	HBA	HBD	LOGP	Lipinski violation
1.	Caffeic anhydride	$C_{18}H_{14}O_7$	342	7	4	2.04	0
2.	Quercetin	$C_{15}H_{10}O_7$	302.23	7	5	1.23	0
3.	Myristic acid	$C_{14}H_{28}O_2$	228.37	2	1	4.45	0
4.	Palmitic acid	$C_{16}H_{32}O_2$	256.42	2	1	4.20	0
5.	Coumaroyl quinic acid	$C_{16}H_{18}O_8$	338.31	8	5	0.05	0
6.	Epiafzelechin	$C_{15}H_{14}O_5$	274.27	5	4	1.20	0
7.	Kaempferol-7-O-Glucoside	$C_{21}H_{20}O_{11}$	447.4	11	5	0.13	0
8.	Betulin	$C_{30}H_{50}O_2$	442.72	2	2	6.39	0
9.	Linoleic acid	$C_{18}H_{32}O_2$	280.45	2	1	4.8	0
10.	Chlorogenic acid	$C_{16}H_{18}O_9$	354.3	9	5	-0.39	0
11.	Luteolin 7-O-rutinoside	$C_{27}H_{30}O_{16}$	610.52	10	3	2.39	1
12.	4 Feruloyl-5- caffeoylquinic acid	$C_{26}H_{26}O_{12}$	530.5	12	6	1.32	3
13.	Myricetin-3-O-hexoside	$C_{21}H_{20}O_{13}$	480.4	13	9	-0.96	2
14.	Apigenin-6-C-glucoside 8C-arabinoside	$C_{26}H_{28}O_{14}$	564.49	14	10	-1.54	2
15.	1,3-Dicaffeoylquinic acid	$C_{25}H_{24}O_{12}$	516.4	12	7	0.83	3

In the present study except the compounds such as Luteolin 7-O-rutinoside, 4 Feruloyl-5- caffeoylquinic acid, Myricetin-3-O-hexoside, Apigenin-6-C-glucoside 8C-arabinoside and 1,3-Dicaffeoylquinic acid all other compounds expressed were found to be highly drug like.

4.2.5. ADMET Properties

The chosen compounds underwent further assessment to examine their drug-like characteristics. This involved analyzing pharmacokinetic parameters necessary for absorption, distribution, metabolism, excretion, and toxicity (ADMET) using PKCSM (Table IX). The predicted values of the active compounds of *H. auriculata* root were compared with the normal range of predicted parameters of ADMET. Overall, all the compounds showed significant ADMET properties that enable every compound to be defined as drug like and non-toxic.

Table IX. ADMET properties

Pharmacokinetic properties		C 1	C 2	C 3	C 4	C 5	C 6	C7	C8	C9	C10	Unit
Absorption	Water solubility	-3.1	-2.95	-4.95	-5.56	-2.96	-2.96	-3.25	-2.55	-5.44	-5.86	log mol/L
	Human intestinal Absorption (HIA)	67.34	77.20	92.69	92.01	30.30	27.57	91.48	32.93	94.53	92.32	% Absorbed
	Skin permeability	-2.73	-2.73	-2.70	2.711	-2.73	-2.73	-2.73	-2.73	-2.7	-2.7	Log Kp
	P-glycoprotein Substrate	N	N	N	N	N	N	N	N	N	N	Yes/No
	BBB permeability	0.11	1.09	-0.02	-0.11	-1.98	-1.34	-0.81	-1.35	-0.29	-0.14	log BB
	CNS permeability	-1.11	-1.06	1.92	-1.81	-0.84	-1.62	-1.74	1.90	-1.03	-1.6	log PS
Metabolism	CYP2D6 substrate	Yes	Yes	Yes	Yes	Yes	No	No	Yes	No	Yes	Yes/No
	CYP3A4 substrate	Yes	Yes	No	Yes	No	Yes	Yes	Yes	Yes	Yes	Yes/No
	CYP2D6 inhibitor	No	No	No	No	No	Yes	Yes	No	No	No	Yes/No
	CYP3A4 inhibitor	No	No	No	Yes	Yes	Yes	Yes	No	No	No	Yes/No
Excretion	Total clearance	0.11	0.40	1.69	1.76	-0.05	0.44	0.25	0.56	0.23	1.933	log ml/min/kg
	Renal OCT2 substrate	Yes	Yes	No	No	No	No	Yes	No	Yes	No	Yes/No
Toxicity	AMES toxicity	No	No	No	No	No	No	No	No	No	No	Yes/No
	Maximum tolerated dose (Human)	-0.2	0.49	0.55	0.70	0.56	0.48	0.13	0.51	0.79	-0.8	log mg/kg/day
	hERG inhibitor	No	No	No	No	No	No	No	No	No		Yes/No
	Oral rat acute toxicity (LD50)	2.17	2.47	1.47	1.44	2.56	1.75	2.36	2.59	2.69	1.4	mol/kg
	Hepatotoxicity	No	No	No	No	No	No	No	No	No	No	Yes/No
	Skin sensitivity	No	No	No	No	No	No	No	No	No	No	Yes/No

C1-Caffeic anhydride; C2-Quercetin; C3-Myristic acid; C4-Palmitic acid; C5- Chlorogenic acid; C6- Coumaroyl quinic acid; C7-Epiafzelechin; C8-Kaempferol-7-O-Glucoside; C9-Betulin; C10-Linoleic acid

4.2.6. Bioactive score

Following the physicochemical ADMET properties, the bioactive scores were evaluated. The scores fall in the following ranges: active> 0, moderately active−5.0 - 0.0, and inactive < -5.0. The bioactivity analysis revealed that all the compounds were highly bioactive except myristic acid, 1,3-Dicaffeoylquinic acid, and Apigenin-6-C-glucoside 8C-arabinoside (Table X).

Table X. Bioactivity score of the selected ligands

S. No.	Compounds	GPCR Receptor	Ion channel modulator	Protein Kinase inhibitor	Nuclear receptor	Protease Inhibitor	Enzyme inhibitor
1.	Caffeic anhydride	0.17	0.07	0.22	0.17	0.07	0.22
2.	Myristic acid	-0.02	-0.07	-0.02	-0.07	-0.02	-0.07
3.	Chlorogenic acid	0.27	0.11	0.42	0.85	0.15	0.52
4.	Coumaroyl quinic acid	0.04	0.01	0.10	0.19	0.03	0.16
5.	Betulin	0.77	0.26	0.88	0.52	0.94	0.17
6.	Quercetin	0.21	0.04	0.41	0.85	0.09	0.51
7.	Palmitic acid	0.06	0.19	0.28	0.36	0.25	0.28
8.	Epiafzelechin	0.03	0.47	0.08	0.15	0.02	0.14
9.	Kaempferol-7-O-Glucoside	0.12	0.08	0.52	0.74	0.02	0.53
10.	Linoleic acid	0.14	0.04	0.51	0.73	0.07	0.51

4.2.7. Retrieval of target proteins

Four target proteins such as elastase (1HNE), gelatinase (1QIB), collagenase (2Y6I), glycogen synthase kinase 3β (1Q5K) were retrieved from the RCSB PDB database, their protein symbol, PDB ID, structures and functions are depicted in Table XI. The selection of target protein for wound healing was made through literature survey. Accordingly, the protein structures were retrieved on basis of a number of criteria such as single monomer, less than 2 Å resolution, *Homo sapiens* and single domain in the protein complex. All the 10 ligands chosen from *H. auriculata* root by standardization from druglike properties study were docked against the four chosen wound pathogenic proteins.

Table XI. Target wound pathogenic proteins with their characteristics and Structure

Name of the protein	PDB ID	Role of the protein	3D Structure of the protein
Elastase	1HNE	Degrades elastin which provides strength and recoil to the skin due to oxidative stress in the wound site	
Glycogen synthase kinase-3β (GSK-3β)	1Q5K	GSK-3 phosphorylates -Catenin destabilizes and blocks the Wnt pathway, where the catenin is activated in mesenchymal cells during the proliferative phase of wound healing.	
Gelatinase	1QIB	Reduces the keratinocyte migration in wound	
Collagenase	2Y6I	Modulation of collagenase expression can affect the efficiency of re-epithelialization in circular excisional wounds	

4.2.8. Molecular docking analysis of the ligand with the target proteins

The intricate intermolecular interactions between the ligand and the target protein, was determined using the automated docking program AutoDock 4 (version 4.2.8). This program conducts grid-based ligand docking, considering energetics, and explores favourable interactions between one or more typically small ligand molecules and a typically larger receptor molecule, often a protein. The three-dimensional structure details of the target proteins were obtained from the Protein Data Bank (PDB). Prior to the docking simulations, protein preparation involved the removal of water molecules unrelated to active sites, restoration of the native state, and the addition of hydrogen atoms. The compounds extracted from *H. auriculata* root obtained from LC-MS analysis were docked into the active site of the proteins. A correlation was calculated by binding score. Proteins such as 1HNE, 1Q5K, 1QIB, 2Y6I were interacted with screened ligands from *H. auriculata* root.

Totally 40 *in silico* docking analyses were performed. The entire docked complex was visualized using discovery studio. The hydrogen bonding interactions between the ligands and the proteins were also visualized. The present computational study aimed to find an efficient drug candidate from the *H. auriculata* root which can inhibit the target proteins responsible for the pathogenesis of the wound. The binding energy, which reflects the binding affinity of the selected compounds with the target proteins, is shown in Table XII.

Table XII. Binding energy scores of docked complexes

S. No.	Compound name	Binding energy (Kcal/mol) against wound-healing proteins			
		1HNE Elastase	2Y6I Collagenase	1Q5K GSK	1QIB Gelatinase
1.	Caffeic anhydride	-2.32	-1.55	-3.71	-2.05
2.	Epiafzelechin	-6.46	-5.61	-6.62	-5.86
3.	Coumaroyl quinic acid	-2.69	-4.75	-5.42	-5.23
4.	Palmitic acid	-4.42	-2.43	-4.89	-4.22
5.	Betulin	-6.48	-9.65	-8.11	-7.90
6.	Quercetin	-3.89	-4.96	-6.12	-5.63
7.	Myristic acid	-1.61	-1.56	-2.09	-1.75
8.	Kaempferol-7-O-Glucoside	-6.19	-7.48	-8.19	-8.05
9.	Linoleic acid	-6.39	-7.32	-6.54	-7.96
10.	Chlorogenic acid	-6.45	-7.18	-9.12	-7.90

The results were calculated based on three primary parameters: docking score, hydrogen bond energy, and residual interaction. These parameters were utilized to assess the binding affinity of the ligand with the binding protein. A more negative docking score suggested a strong binding affinity between the ligand and protein. The presence of numerous hydrogen bonds in the structure indicated a favourable binding mode of the ligand to the protein. Additionally, residual interaction identified the specific amino acid on the protein to which the ligand binds. Tables XIII-XVI and Figures 11-14 provide detailed information on the docking score, hydrogen bond, and residue interaction for the top 4 ligand-protein complexes.

4.2.8.1 Docking interaction between betulin and elastase

In the present docking profile of betulin and elastase, two oxy-hydroxy group interactions were observed at residues GLE 193 and PHE 41 of Elastase. The protein's hydrogen atom bonded with oxygen atom from ligand in the distance of 1.60 Å and 3.40 Å respectively. The partial inference from this interaction confirms the bond distances are within the molecular mechanics property. The docking score was -6.48 and number of hydrogen bonds was found to be 2. A docking score of – 6.48 kcal/mol and 2 hydrogen bonds proves the efficacy of betulin in docking elastase (Table XIII and Fig.11).

Table XIII. Docking interaction between betulin and elastase

Protein complex	Amino acid	Protein atom	Ligand atom	H bond Length (Å)	Docking score (kcal/mol)	No of Hydrogen Bonds
Betulin and Elastase	GLE 193	H	O	1.60	-6.48	2
	PHE 41	H	O	3.40		

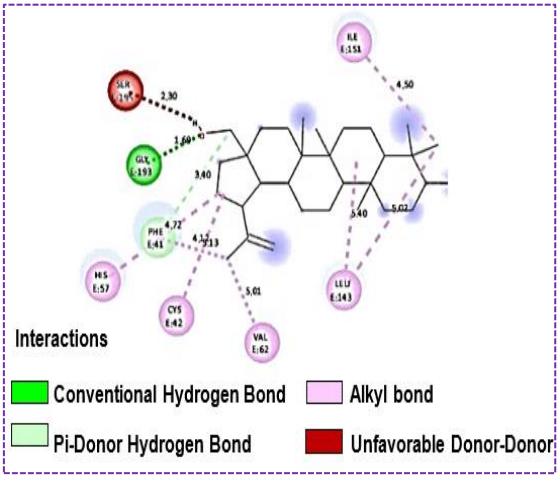

Fig.11. 2D plot of betulin complexed with elastase

4.2.8.2. Docking interaction between betulin and collagenase

The docking profile of collagenase to betulin showed two oxyhydroxy group interaction at residue GLU 268 and PRO 258. The protein's hydrogen atom bonded with oxygen atom from ligand in the distance of 1.20 Å and 3.15 Å. The partial inference from this interaction confirms the bond distances are within the molecular mechanics property. The docking score was -9.65 kcal/mol and number of hydrogen bonds was found to be 2 (Table XIV and Fig.12).

Table XIV. Docking interaction between betulin and collagenase

Protein complex	Amino acid	Protein atom	Ligand atom	Bond Length (Å)	Docking score (kcal/mol)	No of Hydrogen Bonds
Betulin and Collagenase	GLU 268	H	O	1.20	-9.65	2
	PRO 258	H	O	3.15		

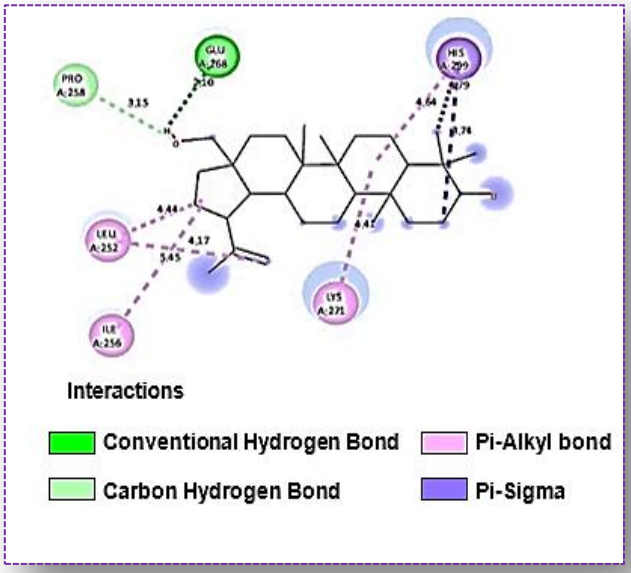

Fig.12. 2D plot of betulin complexed with collagenase

4.2.8.3. Docking interaction between chlorogenic acid and GSK3β

The docking profile of GSK3β to chlorogenic acid showed four oxy hydroxy group interaction at residue ASP 601, SER 602, TRP 604 and PHE 606 of GSK3β. The protein's hydrogen atom bonded with oxygen atom from ligand in the distance of 1.70 Å, 1.97 Å, 2.79 Å and 3.01 Å. The partial inference from this interaction confirms the bond distances are within the molecular mechanics property. The docking score was 9.12 kcal/mol and number

of hydrogen bonds was found to be 4. A docking score of -9.12 kcal/mol and 4 hydrogen bond proves the efficacy of chlorogenic acid in docking GSK3β.

Table XV. Docking interaction between chlorogenic acid and GSK3β

Protein complex	Amino acid	Protein atom	Ligand atom	Bond Length (Å)	Docking score (kcal/mol)	No of Hydrogen Bonds
Chlorogenic acid and GSK**3β**	ASP 601	H	O	1.70	-9.12	4
	SER 602	H	O	1.97		
	TRP 604	H	O	2.79		
	PHE 606	H	O	3.01		

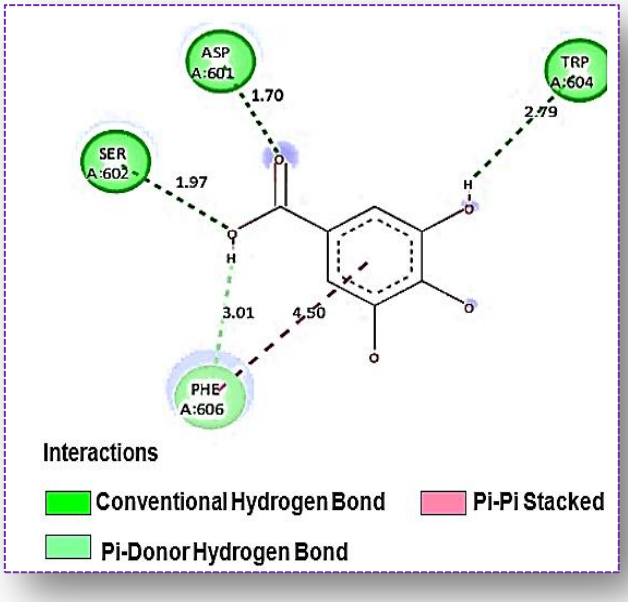

Fig.13. 2D plot of chlorogenic acid complexed with GSK3β

4.2.8.4. Docking interaction between gelatinase and kaempferol-7-O-Glucoside

The docking profile of gelatinase and kaempferol-7-O-Glucoside showed three oxy-hydroxy group interaction at residue ASN 213, GLU 211, GLY 210 of Gelatinase. The protein's hydrogen atom bonded with oxygen atom from ligand in the distance of 2.20 Å, 2.16 Å, 3.25 Å. The partial inference from this interaction confirms the bond distances are within the molecular mechanics property. The docking score was -8.05 and number of hydrogen bonds was found to be 3. A glide score of -8.05 and 3 hydrogen bond proves the efficacy of Kaempferol-7-O-Glucoside in docking Gelatinase (Table XVI and Fig.14).

Table XVI. Docking interaction between kaempferol-7-O-Glucoside and gelatinase

Protein complex	Amino acid	Protein atom	Ligand atom	Bond Length (Å)	Docking score (kcal/mol)	No of Hydrogen Bonds
Kaempferol-7-O-Glucoside and Gelatinase	ASN 213	H	O	2.20	-8.05	3
	GLU 211	H	O	2.16		
	GLY 210	H	O	3.25		

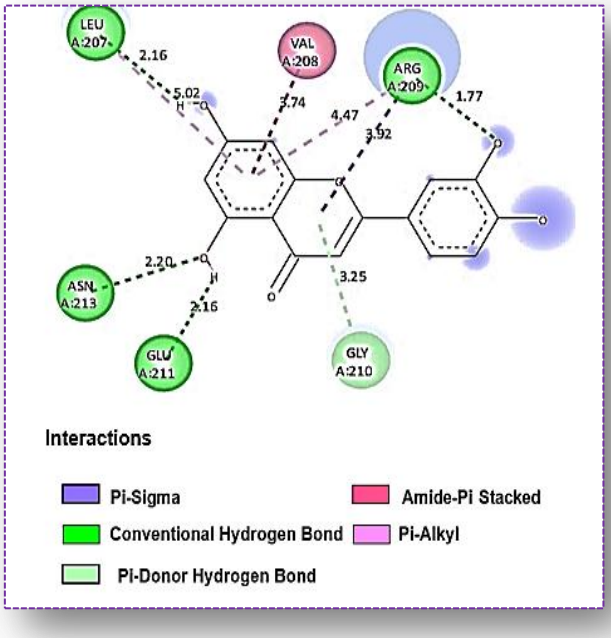

Fig.14. 2D plot of kaempferol-7-O-Glucoside complexed with gelatinase

Overall, the compound betulin showed the highest binding affinity with the wound healing target proteins. The ADMET properties also showed significant results for betulin. Additional to the ligands the protein present in the *H. auriculata* was analysed with its structure and evaluated for docking.

PHASE III

4.3. Liposome synthesis and characterization

Overall, the compound betulin displayed the strongest ability to bind with the protein associated with wound formation. Additionally, betulin exhibited noteworthy results in terms of its pharmacokinetic and safety properties, as indicated by the ADMET analysis. This suggests that betulin is a promising candidate for the development of wound healing drugs. As a result, commercial betulin was employed in further research. Furthermore, the terpenoid betulin was also compared with the *H. auriculata* root for its potential in wound healing studies. The compound betulin as well as the *H. auriculata* root extract was encapsulated in the liposome and evaluated for its comparative wound healing efficiency.

4.3.1. Synthesis of liposome using *H. auriculata* root and the compound betulin

The ethanol extract from the roots of *H. auriculata* and liposomes loaded with betulin were synthesized by the thin film hydration method, which involved sonication. Lipoid P 30 (lecithin) and dichloromethane were utilized in a molar ratio of 2:1 during the process. Thus, formed liposomes were characterized using XRD analysis, TEM analysis, and Zeta potential analysis.

4.3.2. Encapsulation efficiency

In order to determine the encapsulation efficiency of the liposomes UV-Vis Spectrophotometer (Shimadzu Biospec nano) was used. The root extract content in the top and the bottom phase was quantified by comparing the OD with the standard graph. Same method was followed for the compound betulin with the centrifuged supernatant and pellets. The amount of encapsulated root extract in the liposome nanoparticle was found to be 4mg and the amount of encapsulated free nanoparticle was 5.3. Applying these values in the formula, the percentage of EEHA (Ethanol Extract of *H. auriculata*) entrapped in the liposome was calculated as 79.2%. Similarly, for the betulin-encapsulated liposome, the efficiency was found to be 75%. Hence this encapsulation efficiency of 79.2% and 75% EEHA and betulin dispersed in the liposomes was used in the present study.

4.3.3. Spectral characterization of the synthesized liposomes

4.3.3.1. FTIR

The FTIR spectra was done for the samples such as ethanol extract of *H. auriculata* root, liposomes synthesized using *H. auriculata* root extract and liposomes synthesized using betulin. The FTIR pattern was given in the following Fig. 15,16,17. The FTIR profile of ethanol extract of *H. auriculata* root and the liposomes loaded with ethanol extract of *H. auriculata* root was compared. The FTIR spectra of liposomes synthesized using *H. auriculata* root extract reveals various peak which correspond to the following functional groups: a peak at 563.21 cm^{-1} and 601.79 cm^{-1}corresponds to C-Br stretching of Halo Compounds.

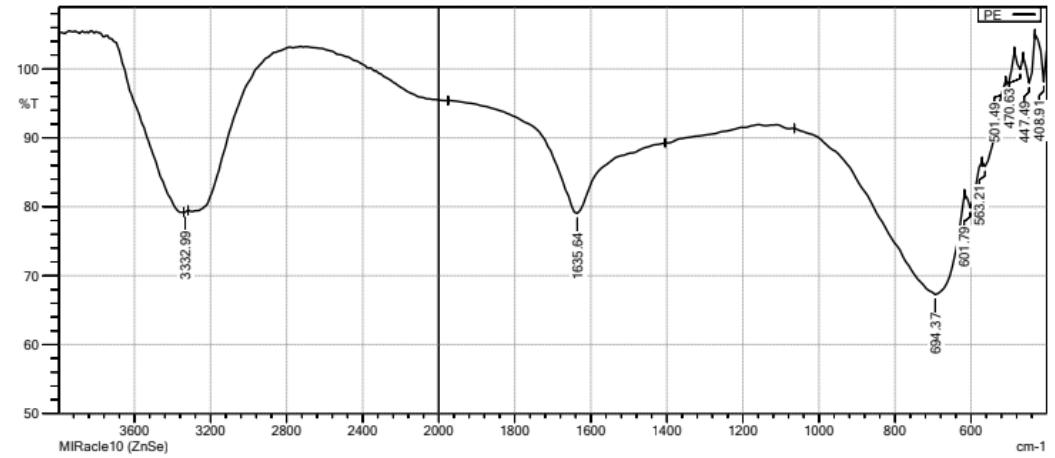

Fig.15. FTIR profile of ethanol extract of *H. auriculata* root

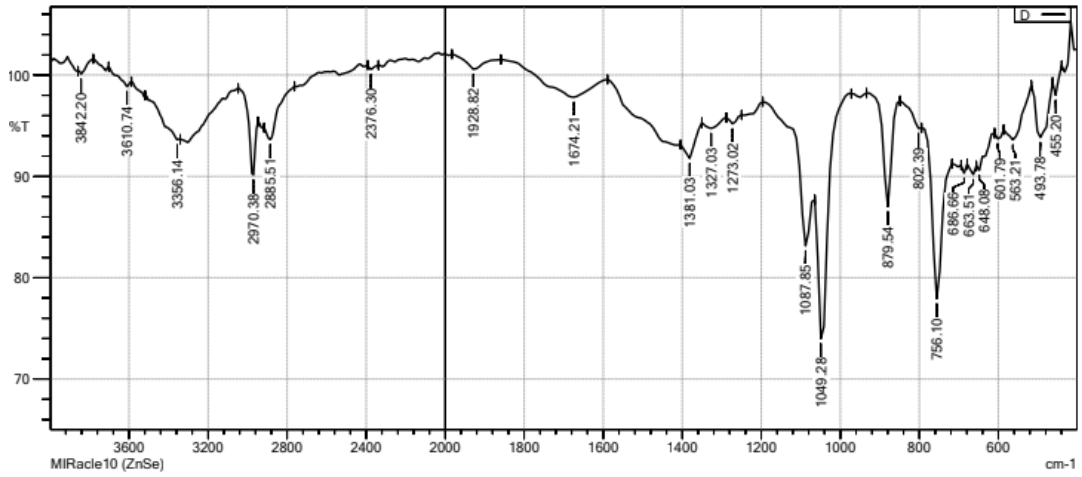

Fig.16. FTIR profile of the liposomes loaded with ethanol extract of *H. auriculata*

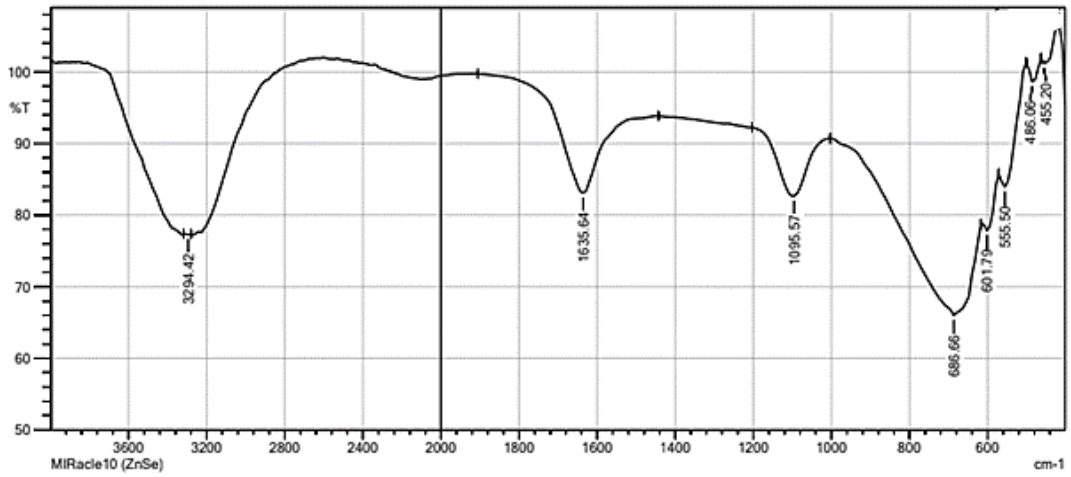

Fig.17. FTIR profile of the liposomes loaded with Betulin

An FTIR spectrum at 879.54 $cm^{-1}$and 1273.02cm^{-1}indicates C=C bending of Alkenes and C-O stretching of Alkyl Aryl Ether. A peak at 1635.64cm^{-1}indicates C=C stretching of Alkene. Peak at 2973.09 cm^{-1} represent C-H stretching of Alkane groups. Peak at 555.50 cm^{-1}represent C-Br stretching of halo compounds. Another peak at 1381.03cm^{-1}indicates O-H bending of phenolic compounds. An FTIR spectrum at 879.54 cm^{-1}indicates C=C bending of Alkenes.1087 cm^{-1} and 3356.14 cm^{-1}represents Strong C-O stretching of Secondary alcohol and O-H stretching of Alcohol. An FTIR spectrum at 879.54 cm^{-1}indicates C=C bending of Alkenes.

4.3.3.2. XRD

The XRD pattern of synthesized liposomes is shown in the Fig. 18 and 19. The diffraction pattern of the liposomes synthesized using *H. auriculata* root extract indicates the existence of Face centred cubic structure (FCC). The high intensity of these diffraction peaks indicates the crystalline nature of the sample where the XRD pattern of the liposomes encapsulated with betulin shows amorphous nature of the sample. Using the 2θ values of the crystalline diffraction pattern, the particle size was calculated using Scherrer equation. The size of the synthesized liposome nanoparticles was 30.35 nm at 2θ=16.3251°, 43.97 nm at 2θ=18.2635°, 12.37 nm at2θ=22.3973°, 75.87 nm at 2θ=23.5971°,25.20 nm at 2θ=23.9646°, 37.59 nm at 2θ=27.4829°, 12.90 nm at 2θ=29.8265°, 27.25nm at 2θ=36.9724 and 13.36nm at 2θ=46.3124 (XRD Crystallite (grain) Size Calculator (Scherrer Equation) –

InstaNANO2022). The mean size was found to be 30.98 nm which is almost similar to the average size obtained using the subsequent TEM analysis.

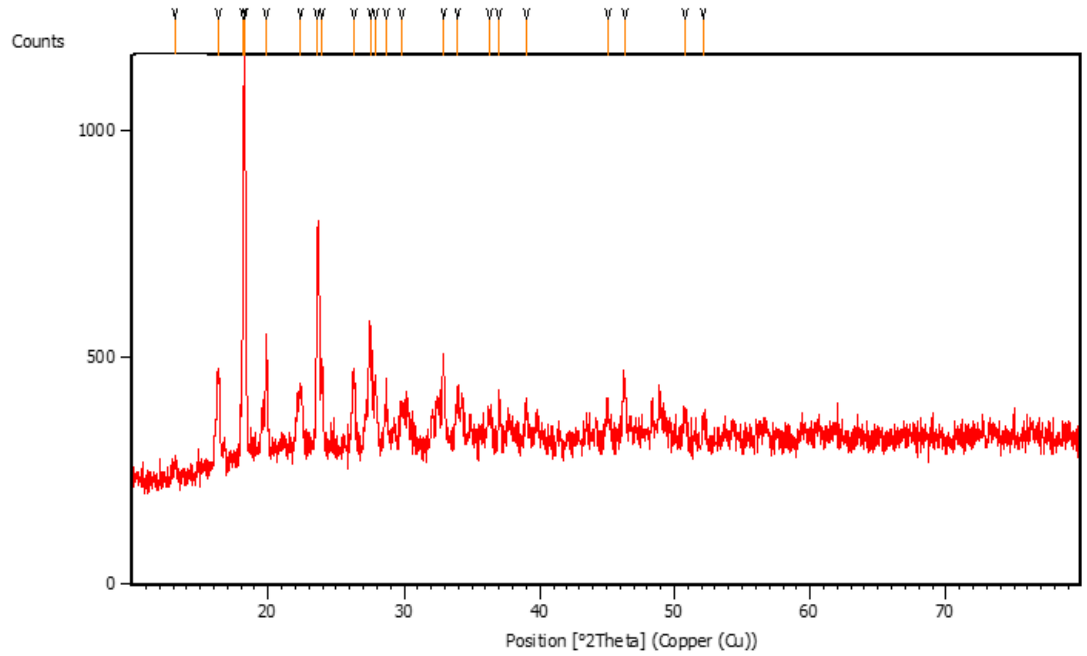

Fig. 18. XRD spectrum pattern of liposomes encapsulated with *H. auriculata*

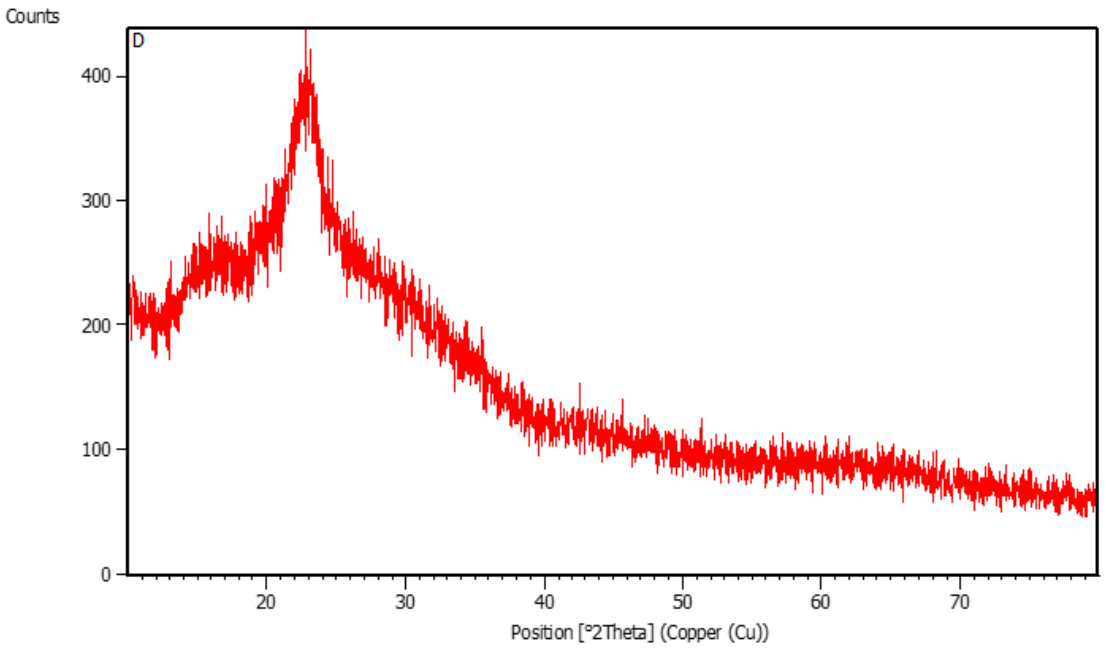

Fig. 19. XRD spectrum pattern of liposomes encapsulated with betulin

4.3.3.3. TEM analysis

TEM is used to analyze morphology, size, aggregation and also nanoparticles distribution. In the TEM analysis of liposomes prepared with *H. auriculata* root extract and betulin, it was noted that the nanoparticles exhibit a size range of 22.655 nm to 37.986 nm and possess a spherical shape (Fig. 20 and 21).

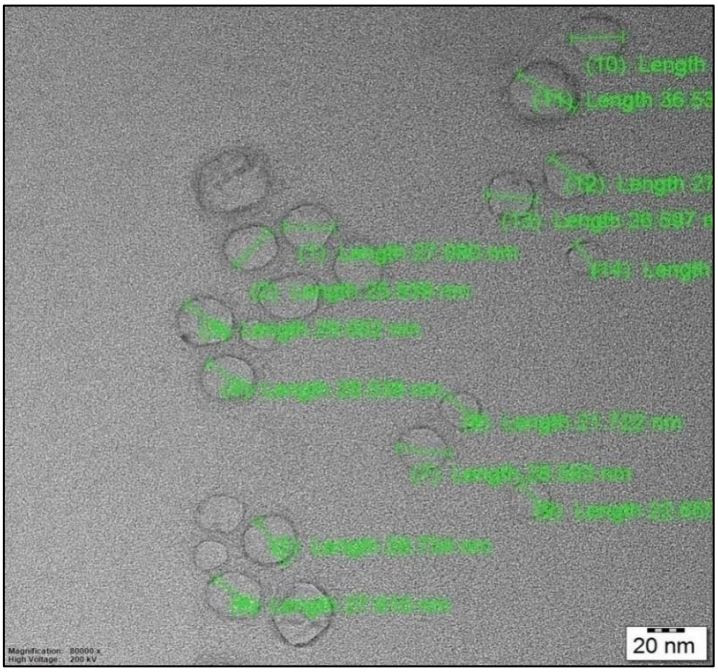

Fig. 20. TEM analysis of liposomes synthesized using *H. auriculata* root

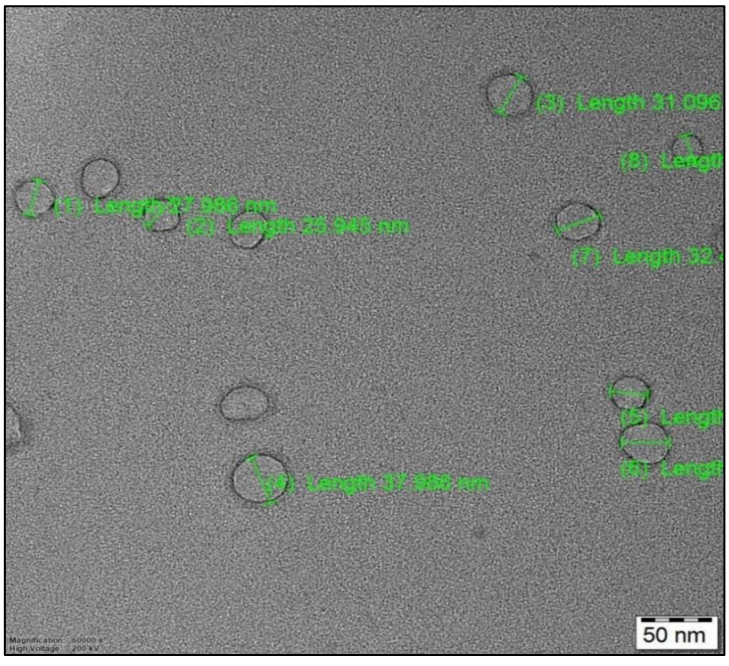

Fig. 21. TEM analysis of liposomes synthesized the compound betulin

4.3.3.4. Zeta potential

The Zeta potential analysis is carried out to analyse the surface charge and colloidal stability of the synthesized *H. auriculata* and betulin liposomes. The zeta potential of the liposomes synthesized using *H. auriculata* root extract was -51.7 mV and for liposomes synthesized using betulin, it was seen to be -0.475 mV where its stability lies in the highest negativity (Fig. 22 and 23).

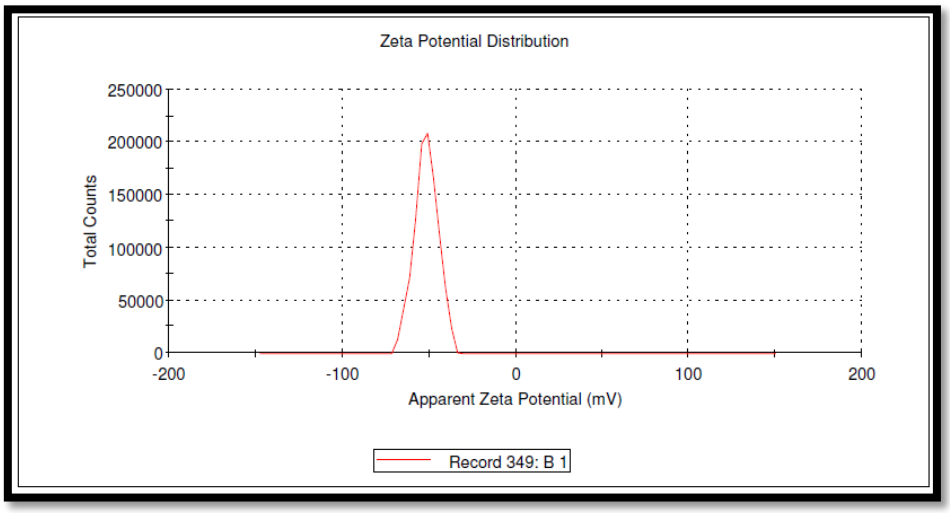

Fig. 22. ZETA potential analysis of liposomes synthesized using *H. auriculata* root extract

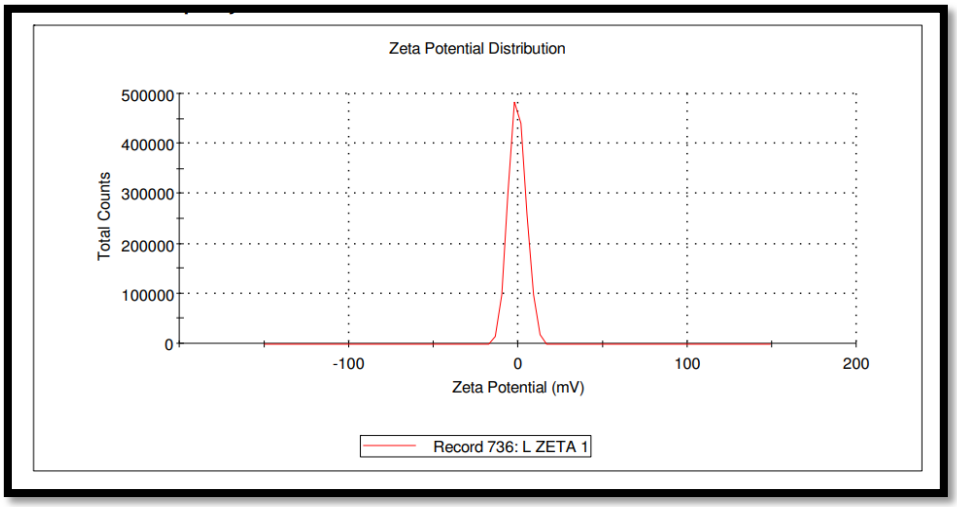

Fig. 23. ZETA potential analysis of liposomes synthesized using Betulin

PHASE IV

4.4. Antibacterial activity, *in vitro* cytotoxicity, wound healing activity and *in vivo* studies

4.4.1. Antibacterial activity

The results of the antibacterial activity are shown in Table XVII. In the present study, the antibacterial efficacy of the bioactive compound betulin and the ethanol extract of *H. auriculata* were assessed before and after the liposome encapsulation. The liposome-encapsulated *H. auriculata* root extract showed the highest inhibition of all the bacterial species compared to all other samples. The values of the zone of inhibition ranged from 12.3 ± 0.57 mm to 22.2 ± 2.3 mm which denotes a much better effect in comparison with control, which is from 18.6 ± 1.15 mm to 27.6 ± 3.2 mm.

Table XVII. Antimicrobial efficacy of liposomes synthesized using *H. auriculata* root extract and betulin without and with liposomal encapsulation

Test organisms	Zone of inhibition in mm				
	EEHA	Betulin	LHA	LB	Control *
Bacillus subtitlis	13.0± 0.57	12.3 ± 1.15	15.3 ± 0.57	14.3 ± 1.0	18.6 ± 1.15
Staphylococcus aureus	18.0 ±1.0	15.8 ± 1.0	18.6 ± 1.52	15.0 ± 1.73	20.0 ± 1.0
Escherchia coli	13.3 ±1.52	12.3 ± 0.57	17.66 ±1.52	16.5 ± 1.73	20.3 ± 1.52
Proteus sp.	13.0 ± 2	14.0 ± 1.0	16.0 ± 1.0	16.3 ±1.0	21.0 ± 1.73

EEHA – Ethanol extract of *H. auriculata*; LHA- Liposome of *H. auriculata*; LB- Liposome of betulin Control- Amoxicillin

4.4.2 Cytotoxicity study

4.4.2.1. MTT assay

The MTT assay was conducted to determine the toxicity of liposome encapsulated *H. auriculata* root and liposome encapsulated betulin using HACAT cell lines. The viability of HACAT cell lines was assessed following treatment with varying concentrations of liposomes (12.5, 25, 50, 100, and 200 µg/mL), with 50 µg/mL of Etoposide serving as the positive control. In the present study HACAT cells showed that the sample concentration is indirectly proportional to the cell viability. When the sample concentration increases, the viability was found to be decreased. The direct microscopic observations of images of liposomes, after incubation were shown in the Fig. 24.

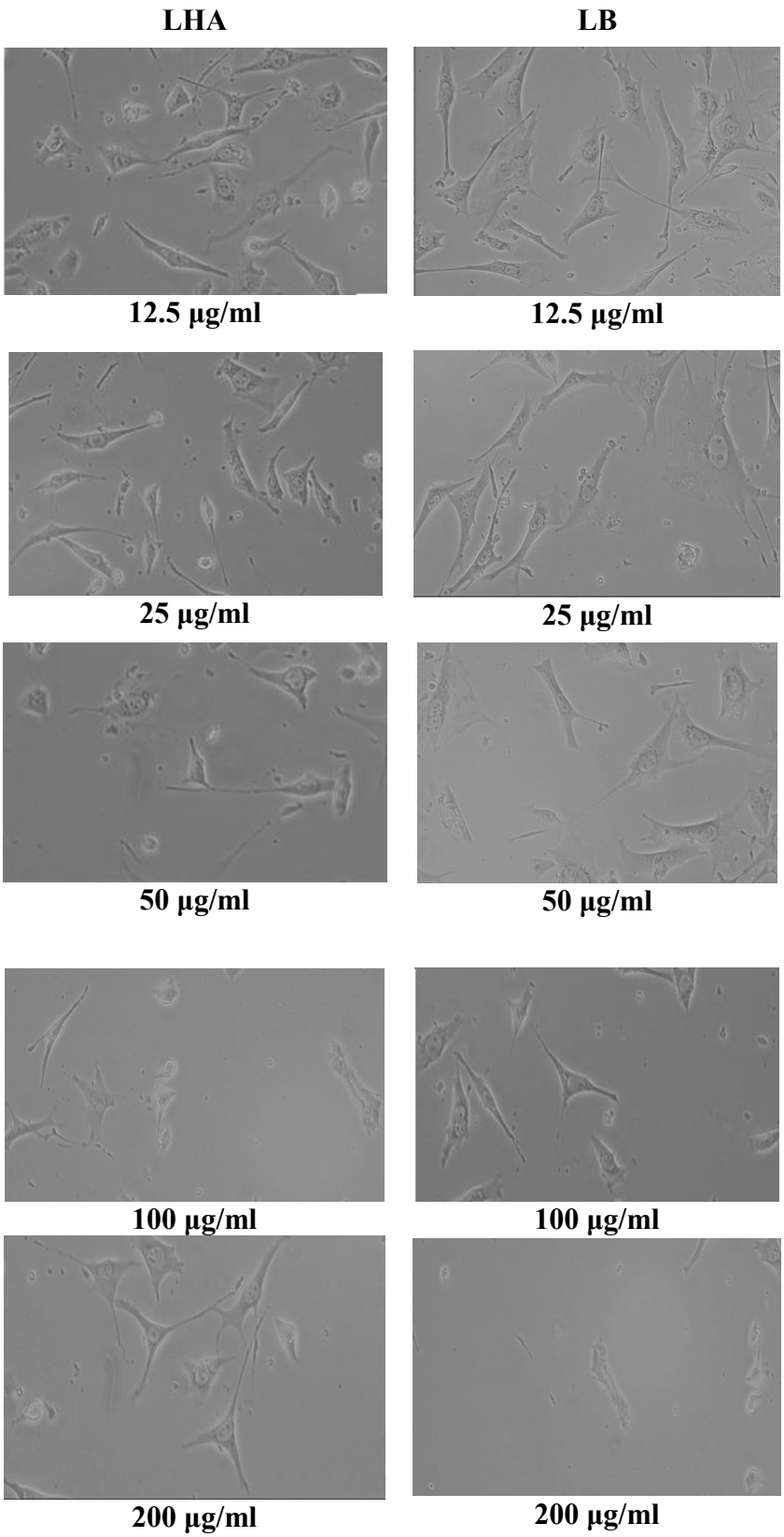

Fig. 24. Cytotoxicity activity of liposomes synthesized using *H. auriculata* root extracts (LHA) and betulin (LB)

Cell viability was comparatively higher in liposome concentrations ranging from 25 to 125 µg/mL when compared to both blank and positive treatments. The cell growth by liposomes synthesized using *H. auriculata* root extract (LHA) and Betulin (LB) was depicted in Fig.25. This suggests that liposomes exert an impact on cell viability and are non-toxic to HACAT cells. Consequently, the 50 µg/mL dose was selected for the scratch assay, as it exhibited minimal reduction in cell viability. The choice of this concentration was driven by the hypothesis that, at 50 µg/mL, diverse outcomes would be observed in the scratch assay test. The IC_{50} value of LHA and LB (LHA- Liposome of *H. auriculata* LB- Liposome of betulin) was found to be 125.77 µg/ml and 97.65 µg/ml. Liposomes synthesized using *H. auriculata* root showed a better cell viability as compared to the liposomes synthesized using betulin.

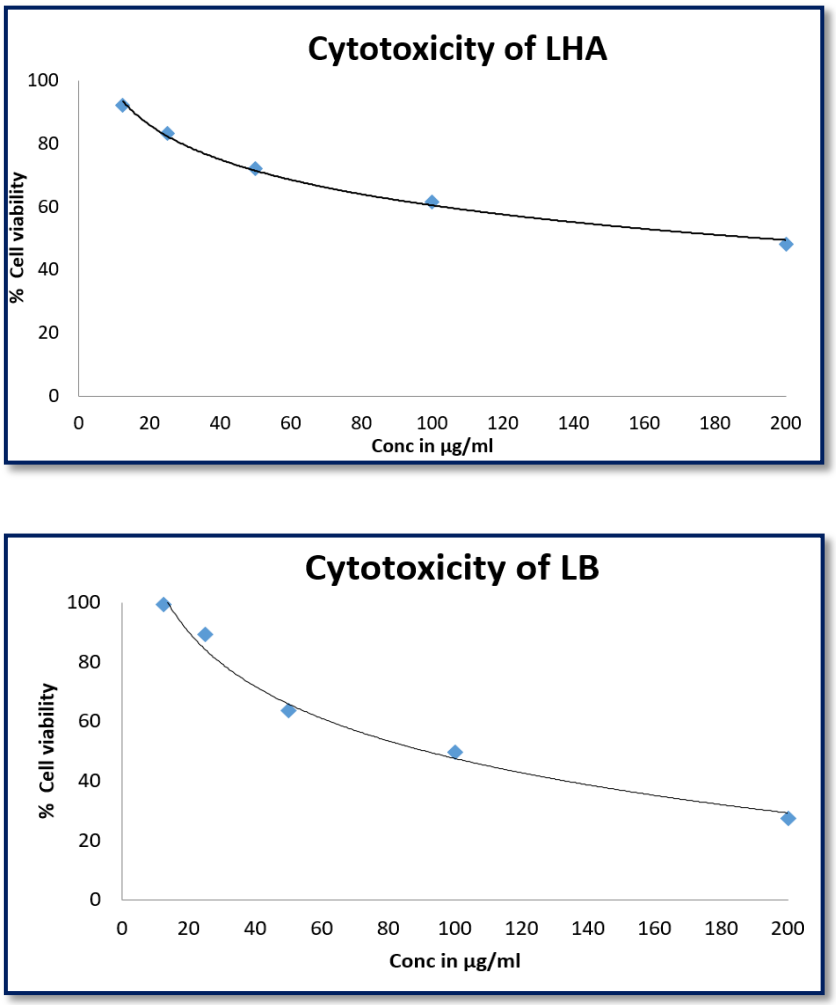

Fig. 25. The cell growth by liposomes synthesized using *H. auriculata* root extract (LHA) and Betulin (LB)

LHA- Liposome of *H. auriculata*; LB- Liposome of betulin

4.4.3. Scratch assay

The results of wound healing assay suggest that both the liposomes have effective healing potency on Human Skin Keratinocytes (HACAT) which decreased the area of wound on incubation dependent manner. The direct microscopic observations of images of liposomes, standard control after 0hour, 24hour and 48hour of incubation are shown in the Fig. 26. A notable rise in cell migration percentage over time was observed in HACAT cells treated with liposomes prepared from *H. auriculata* root, in contrast to those treated with liposomes containing betulin. The cells treated with liposomes synthesized using *H. auriculata* root extract exhibited significantly enhanced migration compared to the cells at 0 hours. The quantified outcomes are depicted in Fig. 27 as a graph illustrating the percentage of cell migration versus time.

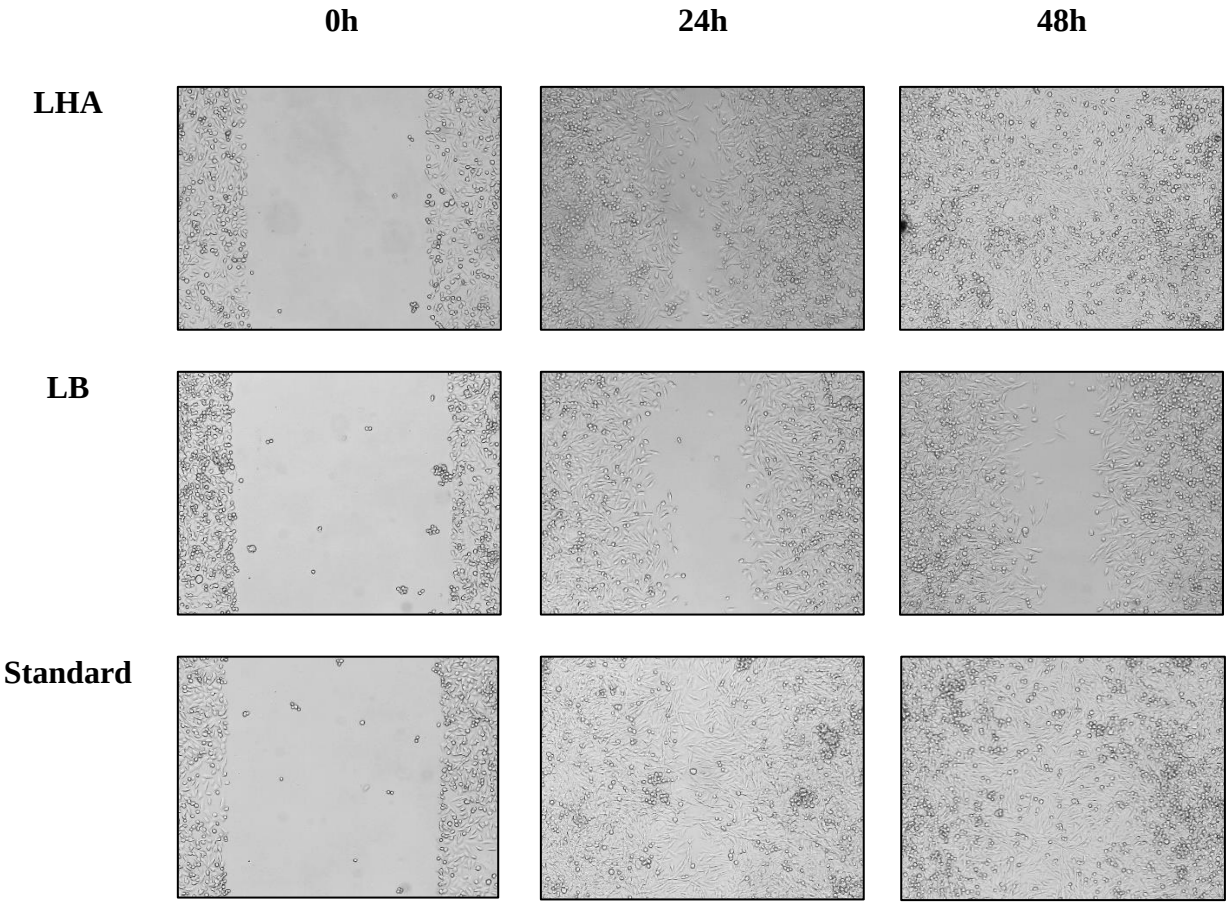

Fig.26. Microscopic view keratinocytes cellular gap closure

LHA- Liposome of *H. auriculata*; LB- Liposome of betulin; Standard- Collagen1

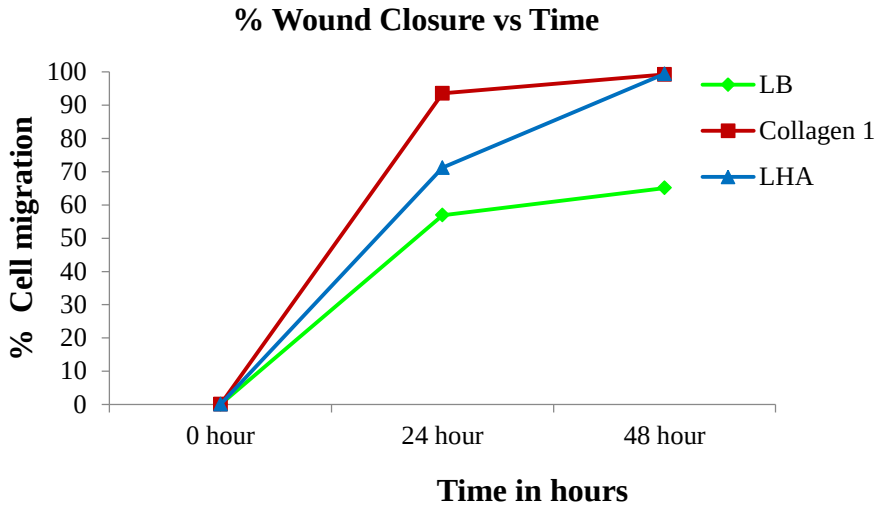

Fig. 27. Graph of percent cell migration versus time

LHA- Liposome of *H. auriculata*; LB- Liposome of betulin; Standard- Collagen1

4.4.3.1. Effect of Liposomes encapsulated with *H. auriculata* treatment on collagen 1 expression

As a followup of scratch assay, the sample demonstrating effective healing was subjected to analysis of collagen 1 expression using flow cytometry. This approach was utilized to evaluate collagen 1 expression in HACAT cells treated with liposomes synthesized using *H. auriculata* root extract and a standard drug.The positive standard control was human Epidermal Growth Factor (hEGF). After 48 hours of liposome treatment, HACAT cells exhibited a significant increase in Collagen 1 expression, comparable to the expression observed in cells treated with the positive control, Collagen 1, as illustrated in Fig. 28. Specifically, 78.35% of HACAT cells treated with liposomes expressed Collagen 1, a percentage closely resembling the expression in cells treated with the standard control, which was 84.89%. This suggests the induction of Collagen 1 expression in HACAT cells by the liposomes.

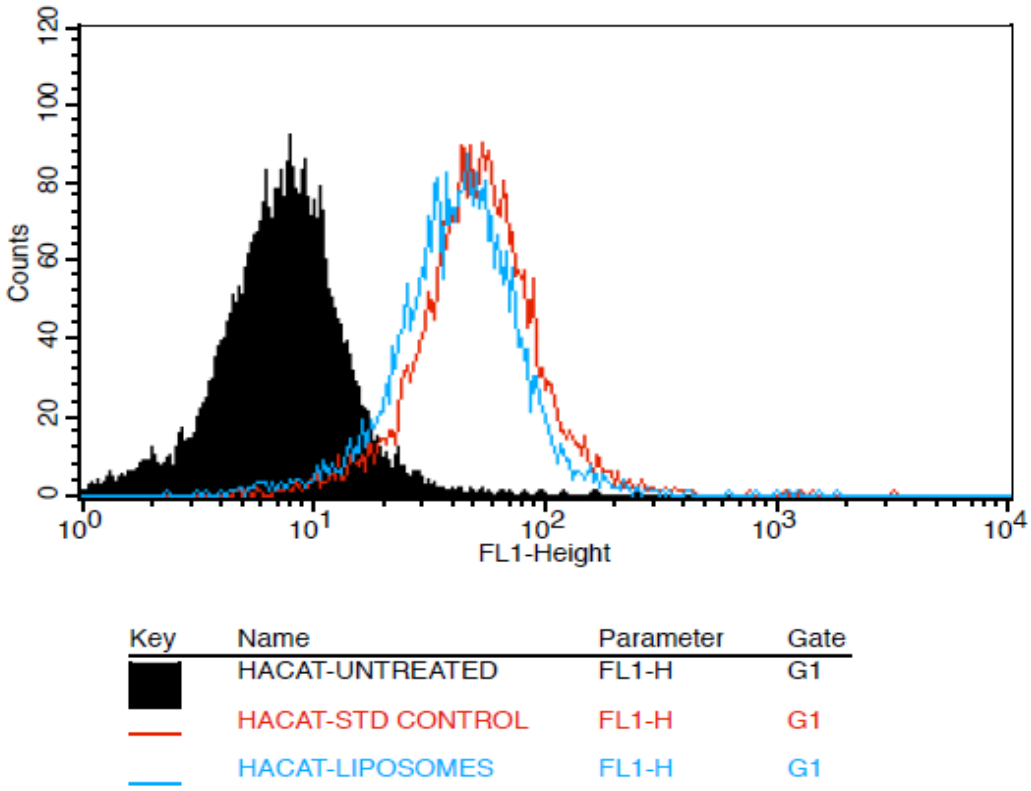

Fig. 28. Collagen 1 expression in HACAT cells by the liposomes

4.4.4. *In vivo* studies

4.4.4.1. Excision model wound healing activity

The wound-healing property of the *H. auriculata* root encapsulated liposomes and betulin encapsulated liposomes was evaluated *in vivo* using excision wound model in Swiss albino rats. The percent wound contraction was evaluated by measuring the changes in the wound area at regular intervals namely, 4^{th}, 8^{th}, 12^{th} and 16^{th} days post wounding in the animal. The result obtained is depicted in Fig. 29 showing the wound contraction. The Table XVIII which shows the wound contraction percentage in the respective treatment days.

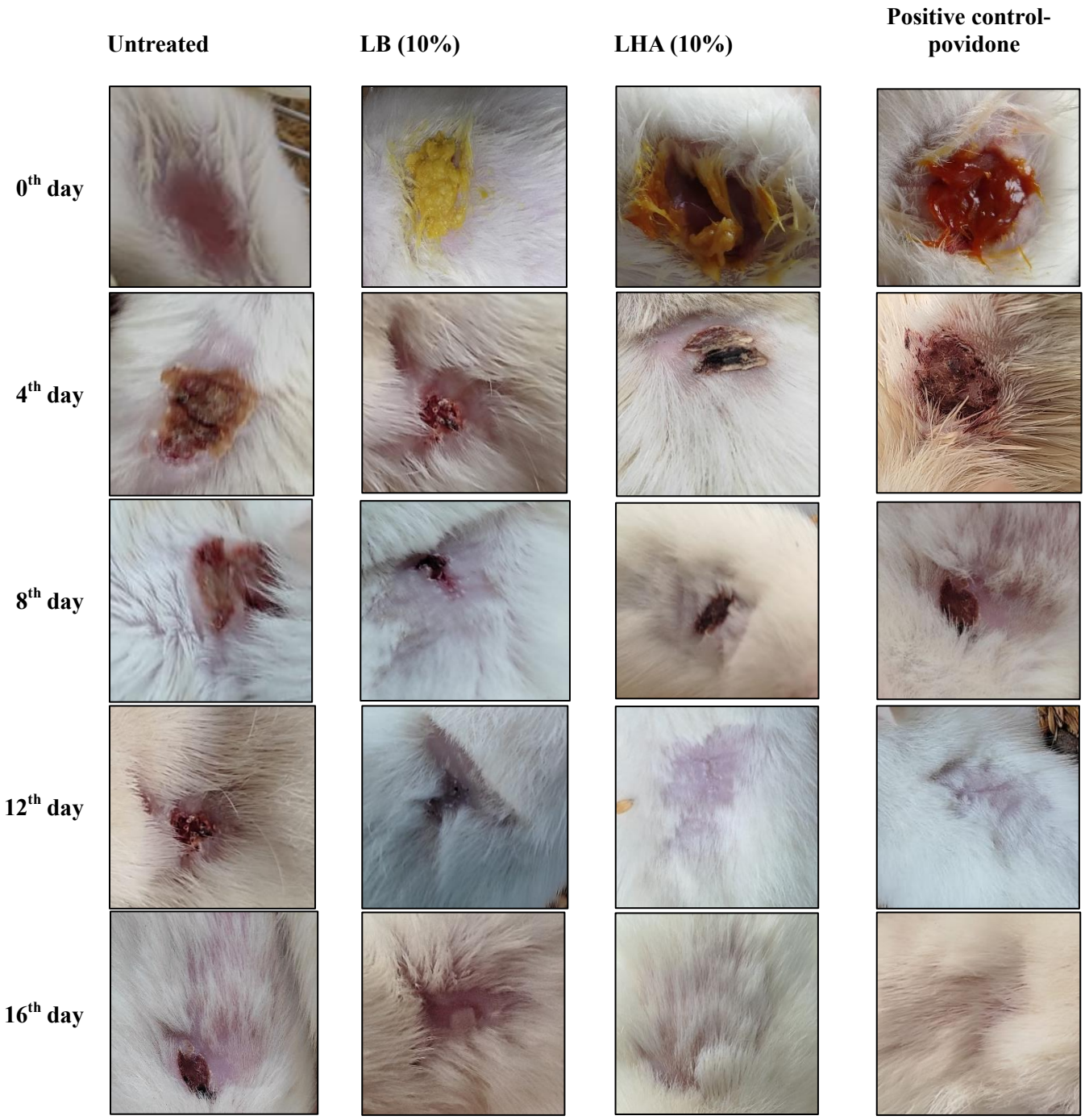

Fig.29. Wound area at regular intervals namely, 4th, 8th, 12th and 16th day

LHA- Liposome of *H. auriculata*; LB- Liposome of betulin

With regard to the wound contraction percentage throughout the experiment period, the contraction was found to be maximum in the treatment with LHA (8±0.47) which was on par with the positive control (10±1.02) whereas the LB treated wound showed contraction percentage of 13±0.27 on day 16. The wound contraction with LB treated animals were delayed on the post wounding days when compared to LHA which shows that LHA treatment is more significant than the LB.

Table XVIII. Wound contraction percentage

Treatments	Day4	Day8	Day12	Day16
Negative control - untreated	105 ± 13.1	102 ±0.70	90.16 ± 0.35	50.37 ± 1.32
Positive control-povidone	90 ± 0.76	58 ± 0.76	27 ± 0.36	10 ± 1.02
LHA	87 ± 0.31	49± 0.60	24 ± 1.21	8± 0.47
LB	92 ± 0.41	62± 0.32	31 ± 0.76	13 ± 0.27
F-test	NS	*	**	**
SEd	0.327	1.256	1.450	2.876
CD	3.795	14.386	1.963	1.986

Values are mean ± SD; n=4 in each group.

****-significant at P<0.01 and *-significant at P<0.05 are compared to control**

NS- Not significant; LHA- Liposome of *H. auriculata*; LB- Liposome of betulin

4.4.4.2. Histopathology

As depicted in Fig. 30, the histological analysis of the healed wound, following treatment with liposomes, revealed a normal-looking epidermis and dermis (B and D). The dermis exhibited an elevated count of blood vessels and inflammatory infiltrate. The wound treated with LB displayed a normal epidermis and dermis, along with normal adnexae. Similarly, the positive control-treated wound exhibited a normal epidermis and dermis, accompanied by an increased presence of blood vessels.

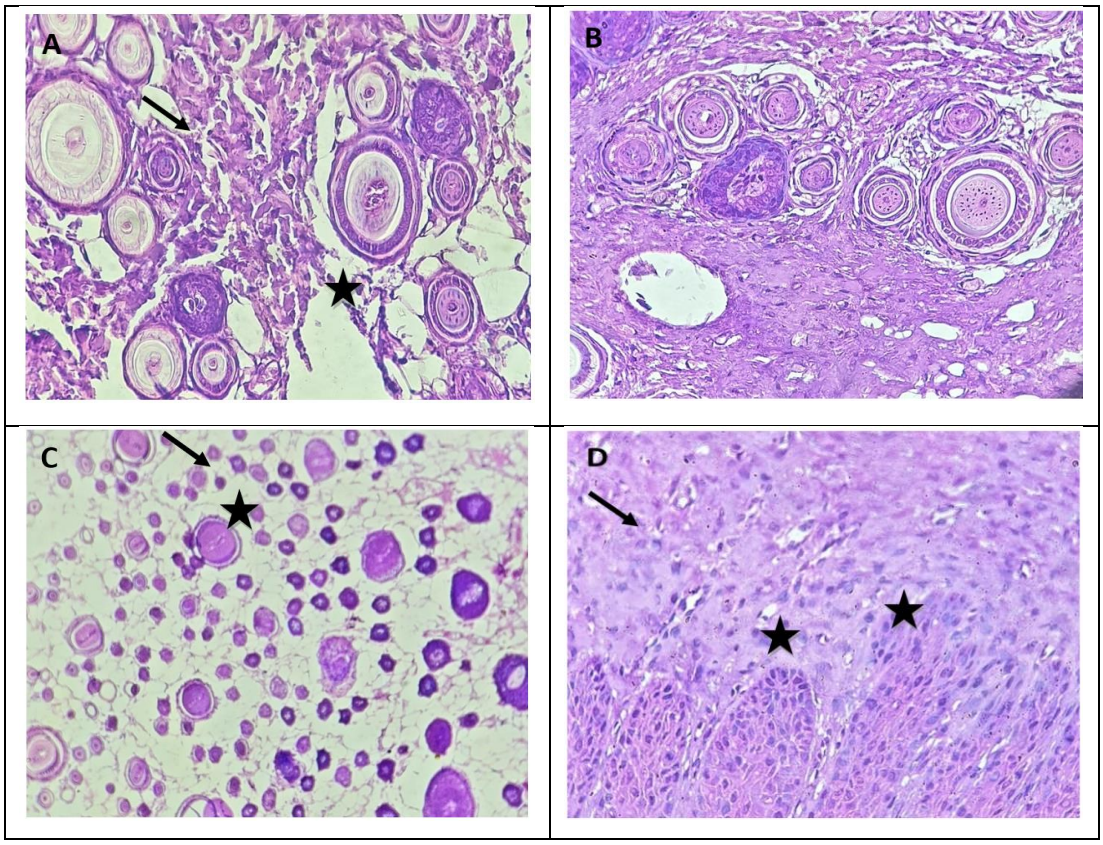

Fig. 30. Histological analysis of the healed wound on treating with liposome showed normal appearing epidermis and dermis

A-Negative control: Moderate dermal congestion (arrow), oedema, inflammatory cells' infiltrations (star★)

B- LB (Liposomes of betulin): Sections studied from the skin biopsy show normal appearing epidermis and dermis. The dermis shows increased number of blood vessels and normal adnexae.

C- Standard-Povidone ointment: Sections studied from the skin biopsy show normal appearing epidermis and dermis (arrow ↘). The dermis shows increased number of blood vessels (star★)

D-LHA (Liposomes of *H. auriculata*): full epidermal re-epithelialisation (arrow↘) in addition to organised tissue formation in the underline dermis; dense thick mature collagen regularly arranged parallel to the regenerated epidermis (star★)

4.4.4.3. Wound healing biomarkers

The analysis of wound healing biomarkers to evaluate healing potential was conducted, and the results are presented in Table XIX.

4.4.4.3.1. Effect of ointment on IL6

With regard to IL 6 content all the treatment groups showed significant decrease when compared to negative control rats. The treatment with LHA and LB to wounded rats reduced IL 6 content to 5700 ± 4.67 pg/ml and 7000 ± 3.20 pg/ml respectively from the untreated control (11,000 ± 1.20 pg/ml). The study was significant at $p < 0.01$ (Table XIX).

4.4.4.3.2. Effect of ointment on CRP

CRP level that generally goes down during the healing of wound and was found to improve in rat treated with LHA and LB (2.87 ± 1.67 and 3.23 ± 1.5) mg/l respectively. LHA treated rats showed more significant result (Table XIX). The maximum reduction of CRP on LHA treated rats was found to be on par with the positive control.

4.4.4.3.3. Effect of ointment on procalcitonin

Total procalcitonin level was found to be the highest in negative control animals 3.95 ± 0.34 ng/ml when compared with the treated rats. Administration of LHA and LB reduced the procalcitonin level to 1.02 ± 0.34 ng/ml and 1.23 ± 0.20 ng/ml respectively which was found to be on par with positive control 0.99 ± 0.21 ng/ml respectively (Table XIX).

Table XIX. Levels of wound healing biomarkers

Groups	IL 6 (pg/ml)	CRP (mg/l)	Procalcitonin (ng/ml)
Negative control - untreated	11,000 ± 1.20	4.5 ± 2.77	3.95 ± 0.34
Positive control-povidone	7000 ± 3.20	3.23 ± 1.5	1.23 ± 0.20
LHA	5700 ± 4.67	2.87 ± 1.67	1.02 ± 0.34
LB	5500 ± 3.05	2.5 ± 1.23	0.99 ± 0.21
F test	**	*	**
SEd **CD**	0.589 3.112	2.346 3.213	2.450 1.212

LHA- Liposome of *H. auriculata*; LB- Liposome of betulin

Values are mean ± SD; n=4 in each group

****-significant at P<0.01 and *-significant at P<0.05 are compared to control**

4.4.4.4. Haematological parameters

The effect of liposome ointment on haematological parameters such as macrophages, neutrophils, Tlymphocytes, Platelets and ESR are presented in Table XX.

4.4.4.4.1. Effect of ointment on macrophages

Between two treatments, the maximum reduction in macrophages was found to be in LHA (2.5 ± 1.60 %) which was on par with the positive control (2.2 ± 1.34 %). The macrophages show a rise in control rats which was then significantly restored to normal on treatment with LHA and LB as the positive control.

4.4.4.4.2. Effect of ointment on neutrophils

With regard to neutrophil count, a significant level in LHA and LB treated rat were tested. Treatment with LHA and LB changed to the normal range values (Table XX). There was a significant decrease in LHA treated rats (58 ± 1.23 %) when compared to the LB (57 ± 1.24 %) treated rats which was on par with the positive control (55 ± 1.34 %).

4.4.4.4.3. Effect of ointment on T Lymphocytes

T Lymphocyte count that generally rises during the occurrence of wound (61± 1.11 %) was found to reduce in rat treated with LHA (57 ± 1.24 %). LHA showed more significant result when compared to the LB which is more nearer to the positive control (Table XX).

4.4.4.4.4. Effect of ointment on platelet count

With regard to platelet count all the treatment groups showed significant decrease when compared to negative control (563± 1.45) 10^9/L. The treatment with LHA reduced the platelet count to 493± 3.24 which was found to be on par with positive control (465 ± 4.11 10^9/L). The study was significant at $p < 0.05$ (Table XX).

4.4.4.4.5. Effect of ointment on ESR

The ESR level was analysed in all the experimental groups of animals. In the negative control group, ESR level was found to be 18 ± 1.03 mm/hr. In the case of LHA treated rats ESR level was found to be reduced to 13 ± 1.14 mm/hr, which was statistically significant at $P<0.05$.

Table XX. Haematological parameters

Groups	Macrophages (%)	Neutrophils (%)	T Lymphocytes (%)	Platelets (10^9/L)	ESR mm/hr
Negative control - untreated	4 ± 3.20	24 ± 1.82	61± 1.11	563± 1.45	18 ± 1.03
Positive control- povidone	2.2 ± 1.34	15.2 ± 1.54	55 ± 1.34	465 ± 4.11	12 ± 2.04
LHA	2.5 ± 1.60	17 ± 2.35	57 ± 1.24	493± 3.24	13 ± 1.14
LB	3 ± 3.04	19 ± 1.64	58 ± 1.23	520± 2.23	15 ± 1.77
F test	**	**	**	*	*
SEd	0.283	1.312	2.679	3.819	3.890
CD	4.512	5.333	5.210	4.321	5.256

LHA- Liposome of *H. auriculata*; LB- Liposome of betulin

Values are mean ± SD; n=4 in each group

****-significant at P<0.01 and *-significant at P<0.05 are compared to control**